Nitrogen Beams with a National Electrostatics Corporation Alphatross Source and a 5SDH Accelerator

B. Harlow,[1, a)] P. A. DeYoung,[1,b)] and V. A. Bunnell[1]

[1]*Hope College Department of Physics, Holland, MI 49423, USA*

a)Corresponding author: blake.harlow@hope.edu
b)deyoung@hope.edu

Abstract. Over the past 15 years, Hope College has been producing hydrogen and helium ion beams with an Alphatross® ion source and 5SDH Pelletron® tandem Van de Graaff accelerator. The manufacturer stated the possibility of creating nitrogen ions from this source, but Hope College has not, up until now, attempted to do so. By mixing approximately 1% nitrogen into hydrogen source gas, imidogen (NH^-) and amidogen (NH_2^-) ions are created and accelerated through the tandem accelerator. Oxygen and hydroxide beams are also present due to residual water vapor in the source after maintenance. Post acceleration, these ion beams were directed into a scattering chamber by a dipole bending magnet for identification. Alternate beams such as these open up new possibilities for future experiments such as nitrogen implantation.

INTRODUCTION

Hope College has an Alphatross® ion source[1] paired with a 5SDH Pelletron® tandem Van de Graff Accelerator[2]. The Alphatross® ion source is a charge-exchange type source and is marketed and used as a source for negative H and He ions. Many of these sources are in operation around the world because they are a reliable technology for the production of He$^-$ ions, not available from sputter sources, for acceleration by tandem accelerators[3].

The manufacturer of this ion source, National Electrostatics Corporation[4], and Ref. 5 state there is a possibility of creating imidogen (NH^-), oxygen, and hydroxide (OH^-) ions with this ion source. Amidogen (NH_2^-) ions could potentially be made, but N$^-$ ions are unexpected because the ground state electron configuration of this ion is unstable.[6] However, very little exact information about finding and optimizing these alternate beams is given. The process necessary to make these alternate beams was studied. Source gas changes were necessary and a model for the bending magnet was created assuming non-relativistic particles. Although the paths through the beam line are very complex, the underlying principle for the model is that all particles with the same value of mv/qB will take the same path through the focusing and bending magnets. Sample ion source and accelerator settings for various beam species have been found for various beam energies and ions. The magnet current required to bend these beams can be consistently predicted using the model which confirms the identity of each beam. These beams have the potential for being used for nitrogen implantation.

ACCELERATOR DESCRIPTION

The current accelerator at Hope College was installed in 2004.[7,8] Fig. 1 shows a layout of the installation. An Alphatross® ion source creates a plasma using an RF electric field and a magnetic field. Ions are extracted with an axial electric field (probe). The positive ions from the plasma undergo charge exchange as they pass through gaseous rubidium.[1,3] Between the ion source and the low energy entrance to the accelerator, the now negative ions are focused and steered. The focusing and steering elements include a velocity selector (crossed electric and

magnetic field), a vertical electrostatic steerer, and an electrostatic Einzel lens. An insertable Faraday cup is used to measure the low energy beam current. While different ions such as NH$^-$ and NH$_2^-$ will have different speeds and only one will follow the central path through the accelerator, the low-energy Faraday cup cannot distinguish these two ions. The same is true for O$^-$ and OH$^-$ ions. The two velocities are very close and since the Faraday cup is close to the velocity selector, the two species are not significantly separate in space when they reach the cup.
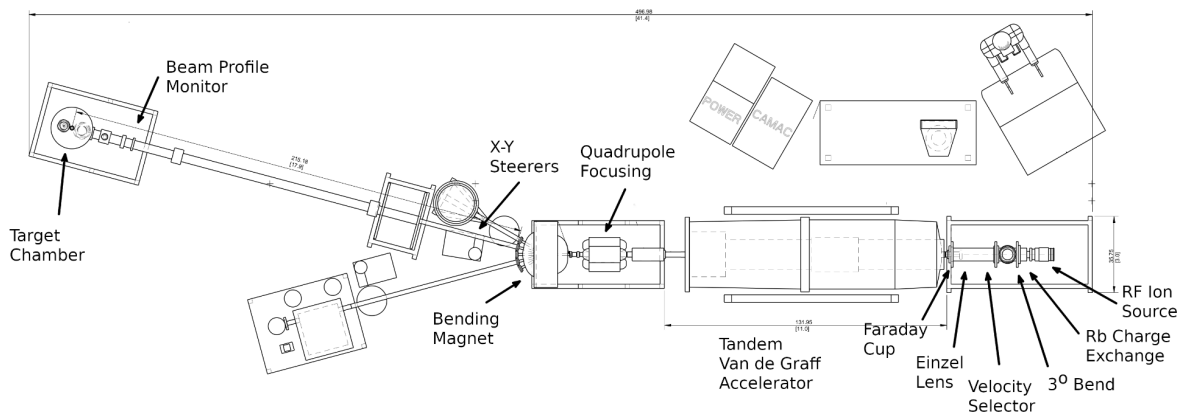

FIGURE 1. Layout of the accelerator and associated components.

The tandem Van de Graff accelerator has a maximum Terminal Voltage (TV) of 1.7 MV. The ions are first accelerated by the positive TV toward the center of the accelerator gaining energy. Electrons are then stripped off during collisions with low pressure nitrogen gas in the center of the tandem leaving a positive ion which is repelled by the TV gaining additional energy. Ions will have a total energy that depends on the TV and Charge State (CS) of the ion after undergoing stripping in the terminal of the accelerator according to $E \approx TV + TV * CS$. This expression is approximate because the ions always have some initial energy from the ion source. Additionally, in those cases where the source produces a molecular ion rather than a simple atomic ion, the expression is even less exact because it does not recognize that the ion has a different mass before and after charge exchange in the center of the accelerator. In general, hydrogen beams will have a maximum energy of ˜3.4 MeV, and α particles (He^{2+}) have a maximum energy of ˜5.1 MeV.

After the accelerator, the beam is directed down a beam line which includes an x and y quadrupole-doublet focusing magnet and a dipole bending magnet. The dipole magnet deflects the beam by 15° into a scattering chamber ˜7.2 m downstream. The x and y magnetic steering magnets on this line were only varied when the particular species and charge state were changed to minimize perturbations to the path. A beam profile monitor is positioned immediately before the scattering chamber and is used to ensure a consistent beam position and shape regardless of beam species and energy. The scattering chamber is equipped with a Faraday cup to measure beam current, and the current in this cup was maximized at each setting to fine tune the beam line settings.

MODELING ION BEAM BEHAVIOR

Approximate ion source settings for imidogen (NH$^-$) are given by the Alphatross manufacturer, but there is only limited documentation regarding specifics. There is little information about exactly what is extracted from the ion source. Specifically, does the source produce atomic nitrogen N$^-$ (unexpected because the extra electron is unbound), molecular NH, molecular NH$_2$ or a combination? In principle, the current in the dipole bending magnet is a sensitive indicator of the energy and species of the accelerated ion, Thus, the main challenge of finding and identifying alternate beams is the need to accurately model the bending magnet behavior.

In general, the behavior of the dipole magnet can be modeled based on Eq. 1,

$$r = \frac{mv}{qB} = K\sqrt{\frac{mE}{q^2I^2}} \, , \tag{1}$$

where m is the ion mass, v is the ion velocity, q is the charge of the ion, and B is the magnetic field in the magnet. Note that, as is frequently the case, the magnetic field is not known, but rather it is the current through the magnet that is known. The goal is to establish a constant path through the bending magnet and then calibrate the current in the magnet with well known ion species and energies.

Eq. 1 can also be cast in terms of E, the total kinetic energy of the ion, I, the current in the magnet coils, and K, a proportionality constant. The proportionality constant is not known because the field for the actual magnet has not been mapped to establish a relationship between the current and the field. However, if ions are constrained to always follow the same path through the magnet, the current needed to bend a reference ion with radius r_0 can be related to the current needed for any other ion following radius r according to Eq. 2.

$$r_0 = r \Rightarrow \sqrt{\frac{m_0 E_0}{q_0^2}} I_0 = \sqrt{\frac{mE}{q^2}} I \tag{2}$$

This can be rearranged as shown in Eq. 3 to predict the appropriate I for any ion given a current I_0 for a specific ion with m_0, q_0, and E_0 that follows a central path.

$$\frac{I}{I_0} = \frac{q_0}{q}\sqrt{\frac{mE}{E_0 m_0}} \tag{3}$$

The process of determining the proportionality constant began with a well-understood reference beam, Hydrogen at 2.513 ± 0.020 MeV. Eq. 3 then gives approximate current values for beams of He and O. If the measured currents are plotted versus $\frac{Em}{q^2}$, the current should show a $y = a + b\sqrt{x}$ behavior. The offset term was included to account for an offset in the current readback from the power supply versus the actual field in the magnet coils.

There is one final consideration that is necessary. When the species leaving the ion source are molecular ions such as imidogen (NH⁻) or hydroxide (OH⁻), these molecules will dissociate in the center of the terminal. In these cases, the energy gained during transit through the accelerator is more complicated because the molecule dissociates when stripping in the terminal takes place. The result is that the final energy of a particle is

$$E_{final} = \frac{m}{M}(|q_i|V_{terminal} + E_{source}) + q_f V_{terminal} \tag{4}$$

where q_i is the charge of the ion extracted from the the source, q_f is the charge after stripping, m is the mass of the species exiting the accelerator and traversing the magnet and M is the mass of the molecule produced in the ion source. The final energies listed in Table I do include the energy given the ions by the extraction voltage in the ion source and the overall bias voltage applied to the source (E_{source}). In this study, no attempt was made to relate measurements to a theory of the dissociation of fast molecular species in matter. There is some theoretical understanding of the dissociation process given in Refs. 9 and 10.

MEASUREMENTS

The bending magnet current for various ions with various charge states and total kinetic energies (various terminal voltages) was adjusted for maximum beam current in the scattering chamber Faraday cup. A summary list of combinations measured is given in Table 1.

The beam-line steerers and the quadrupole doublet focusing magnet were left constant through the range in order to prevent skewing the data by introducing a different path for the particles. A beam profile monitor and a Faraday cup in the downstream scattering chamber were used to find the bending magnet current that gave the maximum beam. The beam profile monitor allowed one to get close to the desired beam location since this visual aid is easier to use and insured that the trajectory was not somehow skewed.

The optimal magnet current and the beam kinetic energy have some uncertainty. The statistical uncertainty in the magnet current was taken to be 0.05 A and reflects the inability of the accelerator operator to find the absolute best setting given the inherent fluctuations in beam current. This uncertainty is smaller than the symbols in the figures shown and discussed below. There is also a systematic uncertainty due to the calibration of the generating voltmeter. This uncertainty is estimated to be ±20 keV and arises because the GVM calibration is done infrequently.

The large dipole bending magnet is subject to hysteresis effects. If hysteresis is ignored when magnet adjustments are made during beam tuning, the relationship between the expected setting and actual setting becomes too imprecise. The size of this effect is shown in Fig. 2. All the measurements presented in the next section were made in a way where the magnet current was always only increased. If the magnet current needed to be reduced, it was turned back to zero before being increased again. Great care was taken when tuning for maximum beam to increase the current in small steps so as not to overshoot the correct current for maximum beam.
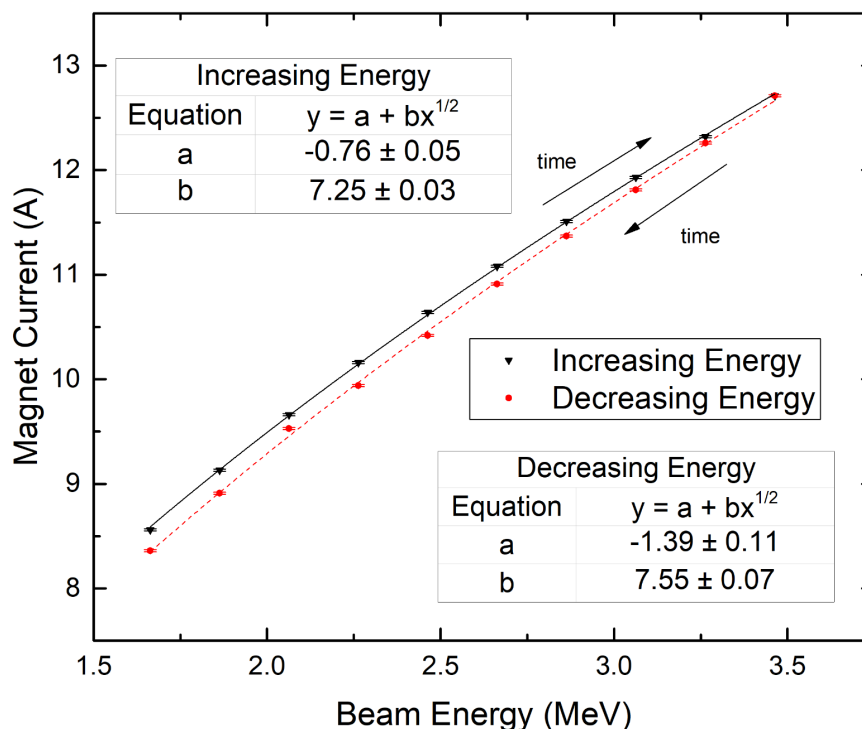

FIGURE 2. Hysteresis in the dipole bending magnet. The solid black line indicates magnet current with increasing energy and the red dotted curve was measured with decreasing steps. (Color on-line)

RESULTS

The goal of this work was to conclusively identify ion beams, especially nitrogen, imidogen, and amidogen from the Alphatross® ion source and transport the resulting beam to the scattering chamber with a usable intensity (>0.3 nA in the scattering chamber). In order to definitively identify the ions, especially those associated with molecules, the systematics of the transport needed to be well understood.

Various combinations of different ions from the ion source, accelerating potentials, and final charge states were directed into the end-station Faraday cup and the magnet current was recorded. Table 1 and Fig. 3 summarize the various combinations that were conclusively identified.

Starting with the H^+ ions of various energies, a preliminary relationship between the magnet current and the parameter $\frac{Em}{q^2}$ was established. The data set was extended to include He^+ and He^{2+} ions of differing energies and final charge states with confidence based on the manufacturer's stated settings in the source operations manual. The relationship was refined and next O^+, O^{2+}, and O^{3+} ions (from atomic O from the source) were added to the data set. The current versus $\frac{Em}{q^2}$ relationship predicted the currents for various final energies and final charge states with

TABLE 1. A summary of the various ion, charge state, and kinetic energy from this investigation. In those cases where a range of energies is given, the typical step size in the accelerator terminal voltage was 100 keV. Also given is the $\frac{Em}{q^2}$ factor from Eq.2 that is necessary to compare the currents for diverse ions.

| Post-source	Final Beam	Final Energy (MeV)	Em/q^2 (MeV×A/Z²)	Magnet Current (A)
H⁻	H⁺	1.67-3.53	1.67-3.53	8.56-12.71
He⁻	He⁺	1.68-3.33	6.71-13.33	17.41-24.79
	He²⁺	2.51-5.30	2.51-5.30	10.58-15.60
NH⁻	N⁺	2.01-3.01	29.15-42.18	36.28-44.26
	N²⁺	3.65	12.79	24.19
	N³⁺	4.89	7.62	18.59
NH₂⁻	N⁺	1.95-2.92	27.34-40.91	35.58-44.37
	N²⁺	3.58	12.54	23.91
O⁻	O⁺	2.50	39.93	43.73
	O²⁺	2.50-5.29	9.98-21.15	21.24-31.44
	O³⁺	3.23-7.05	5.91-12.53	16.31-24.05
OH⁻	O⁺	2.42	38.76	43.02
	O²⁺	2.45-5.18	9.79-20.74	21.01-31.12
	O³⁺	3.27-6.94	5.28-12.34	16.13-23.85
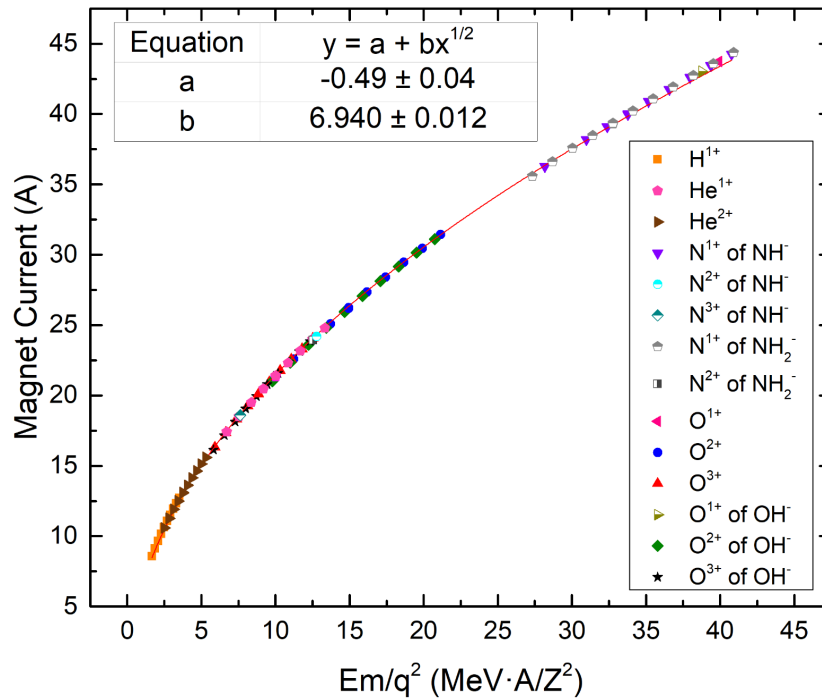
FIGURE 3. Current in the dipole bending magnet for various beams species. The legend shows the variety of initial and final ions, charge states, and molecular species. The x axis, $\frac{Em}{q^2}$, was chosen to account for the obvious main dependencies on mass and charge state allowing all the data to be presented on a single plot. Statistical uncertainties are smaller than the symbol size. (Color online)

reasonable accuracy and the actual measurements were added to the data set. Next, nitrogen ions (N^+, N^{2+}, and N^{3+}) from source ions of imidogen (NH^-) were predicted (Eq. 4) and measured with good accuracy. At this point, weaker beams of N and O from molecular source ions of amidogen (NH_2) and hydroxide (OH) were predicted and measured. No appreciable amount of N^- from the ion source was observed. The final relationship was fit as shown in Fig. 3. The excellent agreement between data and the overall model indicates that usable N beams were produced, accelerated, and properly identified.

Specific ion source settings are given in Table 2. For He measurements, standard He was used as the source gas.

TABLE 2. Ion source settings for the variety of species produced by the ion source.

Ion Species	Source Magnet Current (A)	Probe Voltage (kV)	Bias Voltage (kV)
H^-, NH^-, NH_2^-, O^-, OH^-	4.00	3.00	10.28
He^-	4.00	6.00	17.75

For all other cases, the source gas was 1% nitrogen gas added to the normal hydrogen source gas. The impact of varying this ratio was not investigated. This small admixture of N did not noticeably change the performance of the source when extracting H. It was unnecessary to add oxygen since residual oxygen is prevalent enough in the system simply from oxygen and water vapor introduced into the source when maintenance is done. (The leak rate is low enough that the oxygen beams decrease significantly in intensity during the weeks following source openings.) NEC recommends an aluminum canal for the production of hydrogen ions and the same canal was in place when extracting imidogen and amidogen from the source. It was necessary to adjust the velocity selector, located between the ion source and accelerator, to find maximum beam each time a different species was being extracted from the source. Additionally, a vertical steerer and Einzel lens (also located between the source and accelerator) were adjusted but required only minimal changes. The values of the other source parameters are given in Table 2. The source gas pressure set to the nominal value given by the manufacturer in all cases, ˜3×10^{-6} Torr.

CONCLUSION

The ion species imidogen (NH^-), amidogen (NH_2^-), O^-, and hydroxide (OH^-) species were produced using an NEC Alphatross charge exchange source by incorporating 1% nitrogen into the hydrogen feed gas. Imidogen, amidogen, and hydroxide molecules dissociate in the center of the accelerator terminal in the gas stripper. Atomic N^- ions were not produced at a detectable level as expected.

The measurements are well described by the assumed mathematical model. Additionally, hysteresis was taken into account and analyzed for the dipole bending magnet. These beams have the potential for nitrogen implantation and creating nitrogen vacancies in diamond and other crystalline materials.

ACKNOWLEDGEMENTS

REFERENCES

1. Alphatross Source RF-Charge Exchange Ion Source, https://www.pelletron.com/wp-content/uploads/2017/02/Alphatross-v1.pdf.
2. Complete Pelletron Systems for Ion Beam Analysis, https://www.pelletron.com/wp-content/uploads/2016/09/COMPLETE-IBA-SYSTEM-Handout.pdf.
3. R. Middleton, Nuclear Instruments and Methods in Physics Research **A122**, 35-43 (1974).
4. National Electrostatics Corporation, 7540 Graber Road, P.O. Box 620310, Middleton, WI 53562, USA. nec@pelletron.com. (608) 831-7600.

5. R.J. Ward, G.M. Brown, D. Ho, B.F.O.F. Stockler, C.G. Freeman, S.J. Padalino, and S.P. Regan, CEU poster JP10.00019, 58th Annual Meeting of the APS Division of Plasma Physics, San Jose, CA, USA (2016).
6. H. Hotop and W. C. Lineberger, Journal of Physical Chemistry Reference Data **14,** 732-741 (1985).
7. G. F. Peaslee, and P. A. DeYoung, SM/AE-02, International Topical Meeting on Nuclear Research Applications and Utilization of Accelerators: 4-8 May, Vienna (2009).
8. A. Pena, P. A. DeYoung, and G. F. Peaslee, Poster CK.057, American Physical Society, Division of Nuclear Physics Meeting, Chicago, IL, United States (2004).
9. D. Gemmell, Nucl. Instrum. Methods **179**, 41-56 (1980)
10. J. Remillieux, Nucl. Instrum. Methods **179**, 31-40 (1980).